IEEE Access
Multidisciplinary | Rapid Review | Open Access Journal

Received March 10, 2016, accepted April 1, 2016, date of publication April 7, 2016, date of current version August 4, 2016.

Digital Object Identifier 10.1109/ACCESS.2016.2552078

Layered Multi-Group Steered Space-Time Shift-Keying for Millimeter-Wave Communications

IBRAHIM A. HEMADEH, (Student Member, IEEE), MOHAMMED EL-HAJJAR, (Senior Member, IEEE), SEUNGHWAN WON, (Member, IEEE), AND LAJOS HANZO, (Fellow, IEEE)
University of Southampton, Southampton SO17 1BJ, U.K.

Corresponding author: L. Hanzo (lh@ecs.soton.ac.uk)

This work was supported in part by the European Research Council through the Advanced Fellow Grant: Beam-Me-Up Project, in part by the Engineering and Physical Sciences Research Council under Grant EP/Noo4558/1 and Grant EP/L018659/1, and in part by the Royal Society through the Wolfson Research Merit Award. The DOI for the relevant research data set is: http://dx.doi.org/10.5258/SOTON/390640

ABSTRACT We propose a novel multi-user multiple-input multiple-output (MIMO) technique termed the layered multi-group steered space-time shift keying (LMG-SSTSK) for the downlink of millimeter wave (mmWave) communications, which combines the concepts of multi-user MIMO, space-time shift keying, beamforming and orthogonal frequency-division multiplexing to simultaneously convey information to multiple users. The LMG-SSTSK tackles the propagation challenges of the high-attenuation mmWave frequencies by sub-dividing the users into multiple groups. The proposed system allows more users to be served simultaneously in the downlink over the same time- and frequency-resources than a system dispensing with the proposed grouping technique.

INDEX TERMS MU-MIMO, massive MIMO, millimeter waves, multifunctional antenna array, STSK, OFDM.

I. INTRODUCTION

The large-scale proliferation of wireless communications devices across the globe may lead to a 1000-fold increase in capacity demand over the next decade [1]. The millimetre wave (mmWave) frequency spectrum has recently been considered as a complement to the crowded sub-3 GHz frequency band, since it offers a huge license-free bandwidth (BW) [2]. However, mmWave propagation suffers both from a high path-loss and from sparse multipath scattering [3].

Multiple-input multiple-output (MIMO) techniques have been proposed in the literature both for improving the system's reliability [4] and for increasing the data rates [5]. Additionally, the Signal-to-Noise Ratio (SNR) or Signal-to-interference-Plus-Noise Ratio (SINR) achieved can be improved by beamforming techniques [6]. Intrinsically amalgamating two or more of these compelling MIMO techniques introduces the concept of Multi-Functional Antenna Arrays (MFAA) [7], such as the Layered Steered Space-Time Codes (LSSTC) [8] and Space-Time Shift Keying (STSK) concept [9]. For instance, STSK is capable of striking a trade-off between the attainable multiplexing and diversity gains. MFAAs are capable of simultaneously gleaning the above-mentioned three main MIMO advantages detailed in [7], and the family of mmWave systems more crucially depends on combining these techniques for overcoming their unfavourable propagation characteristics.

Extensive research efforts have been dedicated to single-user mmWave scenarios [10], [11], but recently the community's attention has been shifted towards MU-MIMO systems [12], [13]. Hence in this paper, we introduce a new multi-user system concept conceived for the mmWave frequency band. *The novel contributions presented in this paper are as follows:*

- *We introduce the concept of MU MFAA systems in the downlink of our novel Layered Multi-Group Steered Space-Time Shift Keying (LMG-SSTSK) scheme, which is specifically designed for achieving multiplexing, diversity and hybrid beamforming gains. Our SSTSK concept is a novel multi-user extension of the STSK scheme, where multiple users sharing the same time-and frequency-resources communicate simultaneously.*

- *We present the novel idea of grouping users and partitioning the transmit antennas into layers, where each antenna layer serves a specific group of users. The separation between user groups occurs naturally due to the high attenuation experienced at mmWaves, which is further imposed by highly directional analogue beamforming (ABF). A specific group of multiple users is defined as the set of users who are 1) sufficiently close to each other, so that they fall within the focus of a specific transmitted beam and 2) yet they are sufficiently separated so that they can experience independently fading channels. Partitioning the users into groups and the transmit antennas (TAs) into layers facilitates transmission to a higher number of users compared to a single-layer system having the same number of TAs.*
- *The system also involves digital transmit precoding, where the Multi-User Interference (MUI) of each group's users is cancelled at the transmitter with the aid of digital MU-MIMO transmit precoding (TPC). Furthermore, linear TPC is employed in order to support the above-mentioned digital beamforming and/or to reduce the receiver's complexity, which can be combined with ABF into a hybrid beamforming regime.*

The rest of the paper is organized as follows. In Section II we present the novel concept of our LMG-SSTSK system. Then in Section III we provide simulation results for characterising the proposed LMG-SSTSK system. Finally, we conclude in Section IV.

II. SYSTEM DESIGN

In this section we introduce the LMG-SSTSK system designed for the downlink (DL) of mmWave communications, where we further develop the concept of STSK for the sake of achieving both diversity and multiplexing gains. MIMO techniques are eminently suitable for mmWaves [11], [14], [15], for the sake of mitigating their attenuation and sparse multipath profile [2], [10]. These constraints make beamforming a key enabling technology for mmWave systems [16], in order to mitigate their high attenuation and to reduce the interference among the users in MU-MIMO scenarios.

Again, the above concept of MFAA is adopted to operate at mmWave frequencies for three main reasons. Firstly, to mitigate the high attenuation of the channel by a beamforming gain. Secondly, at say 60 GHz or a wavelength of 0.5 cm we can accommodate a large number of antennas in a relatively small space at the transmitter (Tx) and receiver (Rx). Hence, the degrees of freedom in the system are increased, therefore achieving higher multiplexing gains. Lastly, provided that the antenna elements (AE) can be sufficiently separated at the transmitter and receiver, for achieving their independent fading, MIMO techniques are capable of achieving a beneficial diversity gain. Our design combines STSK with beamforming at mmWave frequencies, hence it is capable of combining multiplexing, diversity and beamforming techniques, whilst striking a trade-off between the first two techniques and having the ability to overcome the high attenuation with the aid of a directional beamforming gain.

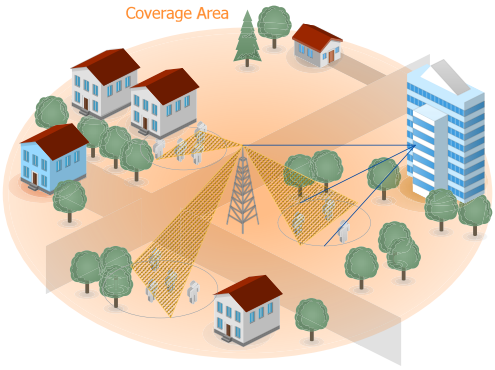

FIGURE 1. A mmWave downlink system having a maximum range of 200 m. Angularly close users form a single user group and are served by a specific transmit antenna layer. As a benefit of the sufficiently high angular separation of all user groups, no interference occurs amongst them.

Given that at mmWaves a large number of compact yet high-gain antenna arrays can be employed [17], narrow directional beams can be utilized for suppressing the interference between the angularly separated[1] users [18], whilst MU-MIMO techniques can be applied to angularly close[2] users that fall within the same transmitted beam, as shown in Figure 1. This in fact is one of the main advantages of mmWaves, where a base station serving a specific user does not interfere with another angularly separated user. However, there is another challenge, since the BS cannot readily communicate with both angularly separated users at the same instant, even if they roam within the same BS's transmission range, since a narrow transmitted beam cannot reach both users at the same time. *Hence, partitioning all users into groups is an efficient technique of increasing the number of users that are being served simultaneously,* as shown in Figure 1. *Explicitly, the system users are divided into three groups, so that the transmitter can communicate with all groups using its layered structure. Furthermore, partitioning the antenna arrays at the transmitter into multiple layers of antenna arrays is an efficient technique of simultaneously serving all angularly separated user groups, where each antenna layer is configured to communicate with all users within the same user group. This introduces the concept of Multiple Groups (MGs) of multiple users.*

The proposed system, which is referred to as Layered Multi-Group Steered STSK (LMG-SSTSK), chooses multiple STSK encoders combined with Orthogonal Frequency-Division Multiplexing (OFDM) for communicating with multiple user groups over mmWaves. Specifically, OFDM

[1] Angularly separated users are users located at sufficiently different angles so the transmitted signal does not reach both simultaneously.

[2] Angularly close users are users located close enough so they fall within the same transmit beam.

is employed in order to overcome the frequency selectivity of the wideband mmWave channel. Furthermore, a group of users can be defined as the set of users, who are sufficiently separated so that they can experience independent fading channels, which can be achieved at a mere few centimetres separation at mmWaves, with the aid of MU-MIMO transmit precoding (TPC) techniques. Users in one group should be angularly close enough so they fall within the same transmitted beam of their assigned transmit antenna layer. The transmitter may then focus the beams of each antenna array layer towards a different user group by employing ABF techniques with the aid of phase shifters and power amplifiers. On the other hand, the users of each group may additionally perform ABF with the aid of their multiple antenna arrays by focusing their receive beams towards the best receive direction.

When the user groups are spaced far enough in order to achieve zero Multi-Group Interference (MGI),[3] the transmitter may communicate with all the user groups with the aid of carefully assigned antenna arrays in a MU-MIMO pattern. The MG system is capable of activating up to two TPC stages prior to transmission: the first stage carries out MU-TPC to cancel the DL co-channel interference imposed on each user group, while the second optional stage eliminates the effect of the DL channel at each UT with the aid of linear DL TPCs to eliminate the effects of the channel at the receiver, which reduces the receiver's design complexity and computational complexity. Furthermore, when all the system's users are angularly close, the system scales down to a single-layer MU-SSTSK.

Symbols used here are as follows: N_G is the number of user groups, N_u denotes the total number of users, $N_{g,u}$ is the number of users per group, $N^t_{c,g}$ is the number of Tx RF chains, X_{g,n_u} represents the STSK codeword of the n_u-th user in the g-th group, W^t_{BB,g,n_u} is the baseband precoding (BBP) matix, D_{g,n_u} is the codeword after applying BBP, W^t_{MU} the MU-TPC matrix, P_{g,n_u} denotes the multiplexed codeword of all users in all groups after applying MU-TPC, F_{g,T_i} is the OFDM group frame, F_{T_i} is the OFDM super-frame, W^t_{RF,T_i} the analogue beamforming TPC matrix, $\hat{H}_{g,n_u}$ represents the channel between the Tx and the user, r_{g,n_u,T_i,n_r} is time domain received signal at the user, n_t is the Tx antenna index, W^r_{BB,g,n_u} denotes the Rx baseband combining, $W^r_{g,n_u,RF}$ is the Rx analogue beamforming matrix and $\bar{R}_{g,n_u}$ is the frequency domain received signal after baseband combining.

A. TRANSMITTER

Consider the downlink of the LMG-SSTSK system shown in Figure 2 combined with OFDM.[4] The BS communicates with N_u users divided into N_G groups as $\{G_1, G_2, \ldots G_{N_G}\}$. The transmitter is equipped with N^t_c RF chain front ends partitioned into N_G layers with a total of N_t AEs.

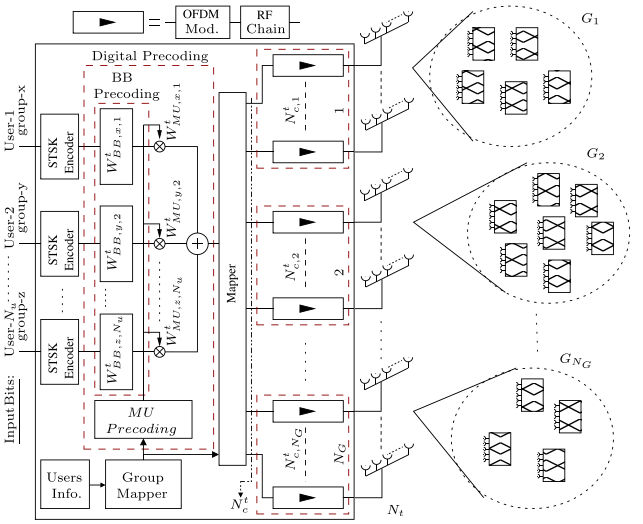

FIGURE 2. LMG-SSTSK transmitter block diagram.

Each g-th transmit antenna layer is formed of $N^t_{c,g}$ RF chain front ends, where $N^t_c = \sum_{g=1}^{N_G} N^t_{c,g}$. The g-th user group contains $N_{g,u}$ users located in the focus of the same transmitted beam, where $N_u = \sum_{g=1}^{N_G} N_{g,u}$.

The LMG-SSTSK transmitter consists of N_u STSK encoders assigned by the group mapper of Figure 2 to serve all users in all N_G groups. Each STSK encoder generates a space-time codeword by spreading $B = \log_2(M_C M_Q)$ bits over T time slots and M spaces,[5] where M_c defines the M_c-PSK/QAM constellation and M_Q denotes the number of dispersion matrices. The LMG-SSTSK codeword is transmitted through an OFDM super-frame [6] over $1, \ldots, T_i, \ldots, T$ time slots. This system is referred to here as LMG-SSTSK(N^t_c, M, N, T, M_Q, M_c).

Assuming that all the N_u users of Figure 2 are grouped into N_G groups and all the input STSK encoders and antenna layers are assigned to their corresponding group, the STSK encoder of the g-th group and n_u-th user generates N_{sc} STSK codewords to be transmitted over N_{sc} sub-carriers and T time slots, where each codeword $X_{g,n_u}(n_{sc}) \in \mathbb{C}^{M\times T}$ is defined as:

$$X_{g,n_u}(n_{sc}) = A_{q,g,n_u}(n_{sc})\, x_{g,n_u}(n_{sc}), \quad (1)$$

$$= [X_{g,n_u,1}(n_{sc}), \ldots, X_{g,n_u,T}(n_{sc})], \quad (2)$$

where $n_{sc} = 1, 2, \ldots, N_{sc}$, the matrix $A_{q,g,n_u}(n_{sc}) \in \mathbb{C}^{M\times T}$ is the dispersion matrix selected from the set $\{A_q\}_{q=1}^{M_Q}$, while x_{g,n_u} is a single M_c-PSK/QAM modulated symbol and $X_{g,n_u,T_i}(n_{sc}) \in \mathbb{C}^{M\times 1}$ is the T_i-th STSK time slot of the $X_{g,n_u}(n_{sc})$ codeword.

The BBP is represented by the $W^t_{BB,g,n_u}(n_{sc}) \in \mathbb{C}^{M\times M}$ matrix, which is then applied to each of the generated STSK codewords to produce the precoded STSK block, as shown in Figure 2. It is termed as the second-stage TPC, because its

[3] MGI defines the level of interference between two user groups.

[4] The LMG-SSTSK combined with OFDM is also termed as LMG-SSTSK, since the system considered in this work is only employed with OFDM so there is no need to differentiate it with a non-OFDM system.

[5] The number of spaces in the STSK encoders is equivalent to the number of antennas in the simplified STSK scheme of [9].

[6] A super-frame here represents the combination of all OFDM symbols transmitted from all antenna layers intended to all users in all groups.

coefficients are extracted after the MU-TPC. The precoded codeword can be expressed as:

$$D_{g,n_u}(n_{sc}) = W^t_{BB,g,n_u}(n_{sc})\, X_{g,n_u}(n_{sc}) \in \mathbb{C}^{M\times T}, \quad (3)$$

where the column representation of $D_{g,n_u}(n_{sc})$ can be defined as

$$D_{g,n_u}(n_{sc}) = [D_{g,n_u,1}(n_{sc}), \ldots, D_{g,n_u,T}(n_{sc})]. \quad (4)$$

Furthermore, in order to suppress the interference between users in the same group, the MU-TPC is employed here and it is based on the *block diagonalization* (BD) technique [19]. In MU-TPC, the precoded codeword $D_{g,n_u}(n_{sc})$ intended for the n_u-th user in the g-th group at the n_{sc}-th sub-carrier is multiplied by an $N^t_{c,g} \times M$ MU-TPC matrix $W^t_{MU,g,n_u}(n_{sc})$ generated by the MU-TPC component of Figure 2, where given that $N^t_{c,g}$ antenna arrays are assigned for transmission to user group g, the MU-precoded codeword is expressed as

$$P_{g,n_u}(n_{sc}) = W^t_{MU,g,n_u}(n_{sc}) D_{g,n_u}(n_{sc}), \quad (5)$$

where all the $N_{g,u}$ multiplexed symbols of all the g-th group's STSK encoders $P_{g,n_u}(n_{sc})$ of the same sub-carrier are summed as:

$$P_g(n_{sc}) = \sum_{n_u=1}^{N_{g,u}} P_{g,n_u}(n_{sc}), \quad (6)$$

and the corresponding symbol at the n_{sc}-th sub-carrier after applying MU-TPC can be expressed as

$$P(n_{sc}) = W^t_{MU}(n_{sc}) D(n_{sc}) = \begin{bmatrix} P_1(n_{sc}) \\ \vdots \\ P_g(n_{sc}) \\ \vdots \\ P_G(n_{sc}) \end{bmatrix}, \quad (7)$$

where $W^t_{MU}(n_{sc})$ and $D(n_{sc})$ are the corresponding MU-TPC matrix and the precoded codewords of all users in all groups, respectively.

Afterward, the N_{sc} symbols are fed into a space-time mapper in order to produce $T \times N^t_c$ OFDM super-frames, where every super-frame holding N_G frames is transmitted simultaneously from the N^t_c antenna arrays over T time slots, as shown in Figure 3(a). Note that $N^t_{c,g}$ should be higher than M, i.e. $N^t_{c,g} > M$. The ST mapper maps the input codewords to the N_{sc} orthogonal sub-carriers. A frame collected during the T_i-th time slot is defined as:

$$F_{g,T_i} = [\bar{P}_{g,T_i}(0), \ldots, \bar{P}_{g,T_i}(N_{sc}-1)] \in \mathbb{C}^{N^t_{c,g}\times N_{sc}}, \quad (8)$$

where $\bar{P}_{g,T_i}(n_{sc}) \in \mathbb{C}^{N^t_{c,g}\times 1}$ is the T_i-th column of the n_{sc}-th multiplexed codeword $P_g(n_{sc})$ of the g-th group frame, as shown in Figure 3(a). Hence, the super-frame at the transmit at time slot T_i is defined as

$$F_{T_i} = \begin{bmatrix} \bar{P}_{1,T_i}(0) & \ldots & \bar{P}_{1,T_i}(N_{sc}-1) \\ \vdots & \ddots & \vdots \\ \bar{P}_{N_G,T_i}(0) & \ldots & \bar{P}_{N_G,T_i}(N_{sc}-1) \end{bmatrix} \in \mathbb{C}^{N^t_c\times N_{sc}}. \quad (9)$$

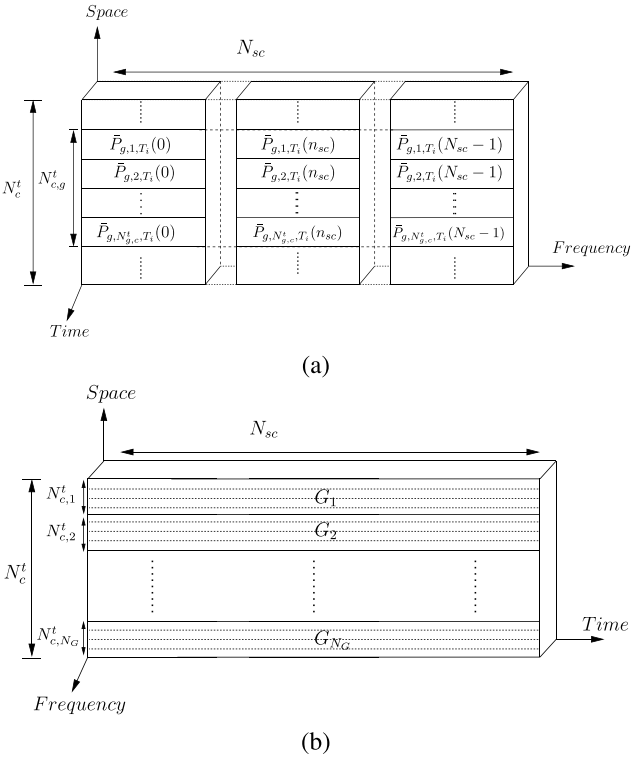

FIGURE 3. (a) The T_i-th time slot OFDM multiplexed frame allocated for the g-th group to be transmitted over the g-th antenna array layer with $N^t_{c,g}$ antenna arrays. (b) The T_i-th OFDM super-frame containing N_G frames.

Moreover, Figure 3(a) shows the g-th frame in the super-frame prior to OFDM modulation. This frame is intended for the g-th group and it contains the multiplexed precoded codewords destined to its corresponding users. The sub-frame, represented by a single row of F_{T_i}, transmitted over the g-th antenna array layer is defined as $\bar{P}_{g,n_t,T_i}[n_{sc}]$, where $\bar{P}_{g,T_i}(n_{sc})$ can be expressed as

$$\bar{P}_{g,T_i}[n_{sc}] = [\,\bar{P}_{g,1,T_i}[n_{sc}], \ldots, \bar{P}_{g,N^t_{g,c},T_i}[n_{sc}]\,]^T. \quad (10)$$

Each g-th frame F_{g,T_i} of the super-frame is fed into its corresponding $N^t_{c,g}$ OFDM modulators in the g-th antenna array layer, where each sub-frame consists of an N_{sc} symbols and can be expressed as $\{\bar{P}_{g,n_t,T_i}(n_{sc})\}_{n_{sc}=0}^{N_{sc}-1}$. Hence, the modulated OFDM symbol array can be expressed as $\bar{p}_{g,n_t,T_i}[n_{sc}] = \sqrt{N_{sc}} \cdot IDFT\left\{\bar{P}_{g,n_t,T_i}(n_{sc})\right\}$, where the super-frame is formed after adding the CP of length N_{cp} at the head of all N_G OFDM symbols.

OFDM modulation is applied to the T_i-th super-frame in order to form the super-frame shown in Figure 3(b), which contains all codewords intended for all users in all groups. The post IDFT-OFDM super-frame is shown in Figure 3(b), where the g-th transmit antenna layer containing $N^t_{c,g}$ antenna arrays transmits a multi-user OFDM-STSK frame intended for all users in the g-th user group, i.e. $N^t_c = \sum_{g=1}^{N_G} N^t_{c,g}$. Each RF chain is connected to a set of N^t_{AA} antenna array elements invoked for performing ABF with the aid of phase shifters and power amplifiers prior to transmission. The number of

arrays in the g-th transmit antenna array layer should be higher than or equal to the sum of all receive antenna arrays for all users in the g-th group, in conjunction with $N^t_{c,g} \geq \sum_{n_u=1}^{N_{g,u}} N^r_{c,n_u}$, where N^r_{c,n_u} is the number of RF chains of the r_{n_u}-th user in the g-th group. The number of antenna arrays of all users is assumed to be identical in all groups, although it is straightforward to generalise the work to any number of users in the different groups.

Finally, RF beamforming is applied at the very end of each RF chain with the aid of phase shifters and power amplifiers. Given that the output of all the N^t_c ODFM modulators at the logical time index n_{sc} is represented by $\left\{\hat{p}_{cp,T_i}[n_{sc}]\right\}_{n_{sc}=-N_{cp}}^{N_{sc}-1}$, the symbol transmitted at the time index n_{sc} can be expressed, without loss of generality, as

$$s_{T_i}[n_{sc}] = W^t_{RF,T_i}[n_{sc}]\hat{p}_{cp,T_i}[n_{sc}], \tag{11}$$

where $W^t_{RF,T_i}[n_{sc}] \in \mathbb{C}^{N_t \times N^t_c}$ is the ABF matrix, which steers each antenna layer to its intended user group, where the g-th antenna layer applies ABF in the direction of the g user group and the $(g+1)$-st antenna array applies its ABF weights towards the $(g+1)$-st user group and so on.

B. USER GROUPING

The most recent efforts on user grouping [12], [13], and [20] exploit the second-order statistics of the channel in order to form user groups. The second-order statistics considered depend on the users' channel covariance matrices. Due to the short wavelengths of the mmWave signal, a large number of antennas may be employed with a compact space to enhance the directivity of the antenna arrays by forming narrow beams. A group of multiple users served by a single base station should be located close enough to fall within the scope of the same transmitted beam.

Local scatterers would to a degree scatter the transmitted signal [2]. For example, in outdoor wireless systems, high rise buildings and landscape structures, may scatter the transmitted signal destined for a specific area [21]. Hence, the users falling within the same geographical area of the incident multipath components would receive a composite signal containing multiplexed data stream for each one of them. The angles of departure and arrivals are considered to be indistinguishable at all receivers, hence the ABF applied at the transmitter is identical for the angularly close users. However, the users should be located far enough so they may experience independent fading. A similar approach was advocated in [12] and [13], where a group was identified as a set of users sharing the second-order statistics, while their instantaneous fading characteristics were assumed to be independent. Furthermore, the angularly close users would apply nearly the same receive ABF weights to the incoming signal, since the directions of the received multipath components are nearly the same at all users.

In this paper, the users are assumed to be grouped into N_G groups, where each group is isolated from the other by the high attenuation of mmWave frequencies. Users within the same group are angularly close enough to fall within the same transmitted beam, and at the same time they are far enough to experience independent fading. At mmWaves, both conditions may be satisfied, since the directional transmit antennas may be focused with the aid of ABF toward a specific area and as little as 5λ spacing between two users is sufficient for the users to experience independent fading channels, which translates to a minimum distance of 10 cm at 28 GHz and 5 cm at 60 GHz.

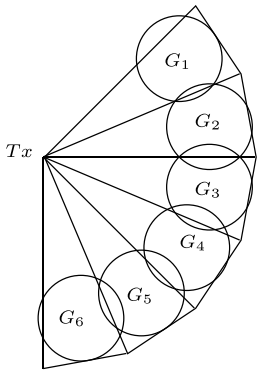

FIGURE 4. Multiple groups belong to multiple transmission sectors.

In addition to the high antenna directionality, the high path loss experienced at mmWaves would further assist us in separating the groups. For example, the two user groups G_1 and G_3 experience zero group interference in Figure 4. When the transmitter beam is focused toward a specific area, the receivers that are far from each other cannot capture the incoming signal due to the associated high attenuations. In LMG-SSTSK, the users are divided into groups based on the sub-sector they belong to, where the sub-sectors are portrayed in Figure 4, and all the users located in the same sector are considered to form a group.

To avoid any inter-group interference, the transmitter does not communicate with two adjacent sectors simultaneously over the same time and/or frequency slot. Conversely, when time-domain multiple group access is considered, the transmit antenna array layers communicate with two angularly separated groups within a specific time slot and with their neighbouring groups in another time slot, we refer to this resource-sharing as the Group-TDMA regime. For instance, consider the 6 groups seen in Figure 4. The Figure illustrates the overlapping between the adjacent groups $G_1\&G_2$, $G_2\&G_3$, $G_3\&G_4$, $G_4\&G_5$ and $G_5\&G_6$, which may lead to inter-group interference. Hence, to avoid this inter-group interference, the transmitter antenna array layers are assigned to cover G_1, G_3 and G_5 during even time slot, as well as G_2, G_4 and G_6 during odd time slots. *The user group-based transmission time slot here should not be confused with the* $1, \ldots, T$ *time slots of the STSK codewords.*

However, when frequency domain multiple group access is considered, a similar approach to that of the MU scheme proposed in [22] may be extended to the multiple group level rather than applying it to multiple users.

The approach of [22] follows the Long Term Evolution Advanced (LTE-Advanced) standard [23], where the Orthogonal Frequency-Division Multiple-Access (OFDMA) concept is adopted for the downlink. Hence, two neighbouring user groups may be served simultaneously by occupying different groups of sub-carriers.

The grouping technique advocated would improve the efficiency of the system by allowing the base station to communicate with more users at any instant than a single-group system.[7] At mmWaves, users should be angularly close enough to be able to receive the same transmitted beam, hence dividing the transmit antenna arrays into layers to simultaneously serve multiple user groups would be an effective mmWave technique.

C. MILLIMETRE WAVE CHANNEL

The mmWave channel is represented by a clustered multipath channel model [25], where a cluster is a combination of many multipath components sharing adjacent space-time characteristics. The channel between a specific transmit antenna element and a single receive antenna element of the n_u-th user in the g-th group can be characterized by a double-directional impulse response of the amalgamate multipath components as [21], [26]

$$\begin{aligned} h_{g,n_u,n_r,n_t}(t,\tau,\theta,\varphi) = \sum_{n_c=1}^{N_{cl}} \sum_{n_p=1}^{N_p(n_c)} & \alpha_{n_c,n_p} \\ & \times \delta(\theta - \bar{\theta}_{n_c}^{Rx} - \theta_{n_c,n_p}^{Rx}) \\ & \times \delta(\theta - \bar{\theta}_{n_c}^{Tx} - \theta_{n_c,n_p}^{Tx}) \\ & \times \delta(t - \tau_{n_c} - \tau_{n_c,n_p}), \end{aligned} \tag{12}$$

where α_{n_c,n_p} is the complex gain of the n_p-*th* multipath component in the n_c-*th* cluster. Both $(\theta_{n_c,n_p}^{Tx}, \theta_{n_c,n_p}^{Rx})$ characterize the (transmit, receive) angle-of-departure (AoD) and angle-of-arrival (AoA), respectively, and $(\bar{\theta}_{n_c}^{Tx}, \bar{\theta}_{n_c}^{Rx})$ are the (transmit, receive) mean cluster angles of the AoD and AoA. The parameter τ_{n_c,n_p} denotes the delay of the n_p-*th* multipath component in the n_c-*th* cluster and τ_{n_c} is the n_c-*th* cluster delay.

Given that each receiver is equipped with N_{r,g,n_u} receive antenna elements, the $\left(N_t \times N_{r,g,n_u}\right)$ discrete-time CIR of the mmWave MIMO channel between the base station and the n_u-th user in the g-th group $\hat{H}_{g,n_u}[n_{sc}] \in \mathbb{C}^{N_{r,g,n_u} \times N_t}$ may be represented as

$$\hat{H}_{g,n_u}[n_{sc}] = \sum_{n_p=0}^{\bar{N}_p-1} \hat{H}_{g,n_u,n_p}[n_p]\delta[n_{sc} - n_p], \tag{13}$$

where $\bar{N}_p = \sum_{n_c=1}^{N_{cl}} \sum_{n_p=1}^{N_p(n_c)} 1$ is the total number of multipath components in all channel clusters and $\hat{H}_{g,n_u,n_p} \in \mathbb{C}^{N_{r,g,n_u} \times N_t}$ is the CIR of n_p-th path, whose entries are denoted by $h_{g,n_u,n_r,n_t}[n_p]$ in order to represent the n_p-th path between the n_t-th transmit antenna of the g-th antenna arrays layer and the n_r-th receive antenna at the n_u-th user in the g-th user group. Furthermore, the channel between the n_g-th antenna layer and the g-th group is null when $n_g \neq g$, since the two groups are well separated, so that the Signal-to-Group-Interference-Plus-Noise Ratio (SGINR [8]) is high enough for ensuring that no interference arrives from the other users. However, for later analysis, the channel $\hat{H}_{g,n_u}[n_{sc}]$ including the effect of the antenna arrays assigned for other groups will be considered.

[7] A single-group system communicates with all users simultaneously as a single group [24].

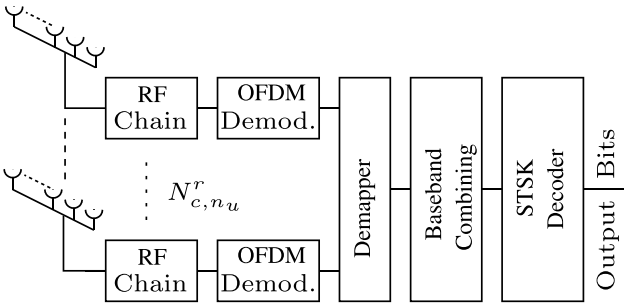

FIGURE 5. LMG-SSTSK receiver block diagram.

D. RECEIVER

The receiver block diagram is shown in Figure 5. The signal received by the n_r-th antenna element of the n_u-th user in the g-th group at the T_i-th time slot is:

$$\begin{aligned} r_{g,n_u,T_i,n_r}[n_{sc}] = & \sum_{n_t=1}^{N_t} \sum_{n_p=0}^{\bar{N}_p-1} h_{g,n_u,n_r,n_t}[n_p] \circledast s_{T_i,n_t}[n_{sc} - n_p] \\ & + v_{T_i,n_r}[n_{sc}], \end{aligned} \tag{14}$$

where $s_{T_i,n_t}[n_{sc}]$ is the corresponding OFDM symbol transmitted from the n_t-th antenna element of $s_{T_i}[n_{sc}]$ defined in (11) and $\circledast$ is the circular convolution operator. ABF is applied at the receiver by directing its receiver beam towards the best receive direction with the aid of power amplifiers and phase shifters. After applying receive beamforming, the signal received at the corresponding users at the n_{sc} time index can be expressed as:

$$\check{r}_{g,n_u,T_i,cp}[n_{sc}] = W^r_{RF,g,n_u}[n_{sc}]\, r_{g,n_u,n_r}[n_{sc}], \tag{15}$$

where $W^r_{RF,g,n_u}[n] \in \mathbb{C}^{N_c^r \times N_r}$ is the ABF matrix of the aforementioned user.

After passing through the RF chains shown in Figure 5, the OFDM demodulators output the detected frequency domain symbol, which is fed into a space-time demapper. After receiving all the T time slots OFDM symbols, the demapper is used to reconstruct the received multiplexed symbols at the n_{sc}-th sub-carrier. The ST demapper takes the n_{sc}-th received vector $\check{R}_{g,n_u,T_i}[n_{sc}]$, which is the frequency domain representation of $\check{r}_{g,n_u,T_i,cp}[n_{sc}]$ after removing the CP by the OFDM

[8] The SGINR determines the level of interference between user groups. When the inter-group interference is zero, its value is equal to the SNR.

demodulators, and constructs the received STSK codewords. Then all received codewords are fed into a baseband combiner, represented by the corresponding sub-carrier's baseband combining matrix $W^r_{BB,g,n_u}(n_{sc})$. Each of the received symbols contains the information intended for all users in the same group, however the MU-TPC suppresses all the intra-group MUI, while the analogue beamforming rejects the other groups' MGI. The symbol at the output of the baseband combiner of the n_{sc}-th sub-carrier can be expressed as:

$$W^r_{BB,g,n_u}(n_{sc})\check{R}_{g,n_u}(n_{sc}) = \{W^r_{BB,g,n_u}(n_{sc})W^r_{RF,g,n_u}(n_{sc}) .\hat{\mathbf{H}}_{g,n_u}(n_{sc})W^t_{RF}(n_{sc})\,P(n_{sc})\} + V(n_{sc}). \quad (16)$$

For simplicity, the sub-carrier index n_{sc} is omitted in the following, hence the above equation is simplified to,

$$\bar{R}_{g,n_u} = W^r_{RF,g,n_u}\check{R}_{g,n_u} \quad (17)$$

$$= W^r_{BB,g,n_u}W^r_{RF,g,n_u}\hat{\mathbf{H}}_{g,n_u}W^t_{RF}\,P + \hat{V}, \quad (18)$$

where $\check{R}_{g,n_u}(n_{sc}) \in \mathbb{C}^{N^r_c \times T}$ is the codeword demapped from the received vectors at the sub-carrier n_{sc} at the n_u-th user in the g-th group after T time slots, $\hat{\mathbf{H}}_{g,n_u}(n_{sc}) \in \mathbb{C}^{N_{g,r_{n_u}} \times N_t}$ is the frequency domain representation of $\hat{H}_{g,n_u}[n_{sc}]$ at the n_{sc}-th sub-carrier, $W^r_{BB,g,n_u}(n_{sc}) \in \mathbb{C}^{K \times N^r_{c,n_u}}$ is the baseband receiver combing matrix at the corresponding user, with K being the received vector's length. The value of K considered here is N^r_{c,n_u}, and $\hat{V}(n_{sc}) \in \mathbb{C}^{N^r_{c,n_u} \times T}$ is the frequency domain noise vector.

Then, after applying the ABF, the RF channel at the n_u-th user in the g-th group can be replaced by the effective channel defined as

$$H_{n_u} = W^r_{RF,g,n_u}\hat{\mathbf{H}}_{g,n_u}W^t_{RF}, \quad (19)$$

where $H_{n_u} \in \mathbb{C}^{N^r_{c,n_u} \times N^t_c}$, hence we have $\bar{R}_{g,n_u} = W^r_{BB,g,n_u}H_{n_u}P + \hat{V}$.

As stated earlier, the MGI is zero, which means that the effect of the interfering symbols intended for users in other groups is eliminated. Hence, the effective channel at the corresponding user is $H_{g,n_u} \in \mathbb{C}^{N^r_{c,n_u} \times N^t_{c,g}}$, which is the channel after applying beamforming between the g-th antenna array layer at the transmitter of size $N^t_{c,g}$ and the n_u-th user's receive antenna array in the g-th group. In LMG-SSTSK, its value is known at the BS. Then, the received signal can be expressed as

$$\bar{R}_{g,n_u} = W^r_{BB,g,n_u}H_{g,n_u}W^t_{MU,g,n_u}D_{g,n_u} + W^r_{BB,g,n_u}\sum_{k\neq n_u}^{N_{g,n_u}}\left\{H_{g,n_u}W^t_{MU,g,k}D_{g,k}\right\} + W^r_{BB,g,n_u}\sum_{n_g\neq g}^{N_G}\sum_{k=1}^{N_{n_g,n_u}}\left\{H_{n_g,n_u}W^t_{MU,g,k}D_{n_g,k}\right\} + \hat{V}, \quad (20)$$

where the intra-group MUI of the users within the same group is suppressed with the aid of MU-TPC. The BD technique [19] is adopted in this paper although any TPC technique can be applied. Then we have $W^r_{BB,g,n_u}\sum_{k\neq n_u}^{N_{g,n_u}}\left\{H_{g,n_u}W^t_{MU,g,k}D_{g,k}\right\} \approx 0$, and the MGI interference is suppressed with the aid of the user grouping and ABF, where our user grouping technique has already grouped the users by ensuring that their MGI is zero and the ABF further focused the transmitted signal towards the intended user group only, hence we have $W^r_{BB,g,n_u}\sum_{n_g\neq g}^{N_G}\sum_{k=1}^{N_{n_g,n_u}}\left\{H_{n_g,n_u}W^t_{MU,g,k}D_{n_g,k}\right\} \approx 0$, which implies that

$$\bar{R}_{g,n_u} = W^r_{BB,g,n_u}H_{g,n_u}W^t_{MU,g,n_u}D_{g,n_u} + \hat{V}, \quad (21)$$

and

$$\bar{R}_{g,n_u} = W^r_{BB,g,n_u}Z_{g,n_u}D_{g,n_u} + \hat{V}, \quad (22)$$

where Z_{g,n_u} is the effective channel defined as $Z_{g,n_u} = H_{g,n_u}W^t_{g,MU,n_u}$. Then

$$\bar{R}_{g,n_u} = W^r_{BB,g,n_u}Z_{g,n_u}W^t_{BB,g,n_u}X_{g,n_u} + \hat{V}. \quad (23)$$

Now, the N_{sc} received STSK codewords are fed into the user's STSK decoder shown in Figure 5, which decodes the received codewords in order to regenerate the transmitted bits. Furthermore, in order to view the system as an extended SM system for each n_{sc} received codeword, the $(KT \times 1)$ received symbol of the equivalent SM can expressed scheme after performing the vectorization operation as:

$$\bar{\mathbf{R}}_{g,n_u} = \mathcal{H}_{g,n_u,n_{sc}} \cdot \chi \cdot \tilde{\mathbf{x}}_{g,n_u,n_{sc}} + \tilde{\mathbf{v}}_{n_{sc}}, \quad (24)$$

where $\chi = [vec(A_1), \ldots, vec(A_{M_Q})]$ is the equivalent $\mathbb{C}^{KT \times N_Q}$ dispersion matrix, $\mathcal{H}_{g,n_u,n_{sc}} = I \otimes \check{H}_{n_u}$ is the equivalent $\left(N^r_{c,n_u}T\right) \times \left(N^t_{g,c}T\right)$ channel matrix of $\check{H}_{n_u} = [W^r_{BB,g,n_u}Z_{g,n_u}W^t_{BB,g,n_u}] \in \mathbb{C}^{N^r_{c,n_u} \times N^t_{g,c}}$ over T time slots, $\tilde{\mathbf{x}}_{g,n_u,n_{sc}}$ is the corresponding n_u-th user's equivalent dispersion matrix selection vector given by $\tilde{\mathbf{x}}_{g,n_u,n_{sc}} = [\underbrace{0,\ldots,0}_{q-l}, x_{g,n_u}(n_{sc}), \underbrace{0,\ldots,0}_{M_Q-q}]$ and $\tilde{\mathbf{v}}_{n_{sc}} = vec\left\{\hat{V}\right\} \in \mathbb{C}^{KT \times 1}$ is the equivalent vectorized noise.

The Maximum Likelihood (ML) detector is applied at the decoder in order to estimate the received codeword at the n_{sc}-sub-carrier over T time slots characterized by $\hat{l}$, which is the estimate of the l-th modulated PSK/QAM symbol and by $\hat{q}$, which denotes the estimate of the q-th transmitted dispersion matrix, and it is given by

$$< \hat{l}, \hat{q} >= \arg\min_{i,j} \parallel \bar{\mathbf{R}}_{g,n_u} - (\mathcal{H}_{g,n_u,n_{sc}} \cdot \chi)_j . x_i \parallel^2, \quad (25)$$

where the symbol x_i is the i-th symbol of the M_c symbol constellations and $(\mathcal{H}_{g,n_u,n_{sc}} \cdot \chi)_j$ is the j-th column of the product matrix $(\mathcal{H}_{n_u,n_{sc}} \cdot \chi)_j$.

E. DIVERSITY ORDER

When BD is employed for MU-TPC, the diversity order of the LMG-SSTSK system can be enhanced, provided that the number of transmit antenna arrays per group is higher than the total number of antenna arrays in the corresponding user group. The diversity order achieved at the n_u-th user can be expressed as

$$\mathcal{D}_{MG} = (N^t_{g,c} - \tilde{\mathcal{R}}_{BD,g,n_u}) \times \min(M,\ T), \tag{26}$$

where $\tilde{\mathcal{R}}_{BD,n_u} \leq \sum_{k\neq n_u}^{N_{g,n_u}} N^{r_k}_{g,c}$. When the channel's correlation is zero, then $\tilde{\mathcal{R}}_{BD,n_u}$ reaches its maximum and the diversity order becomes

$$\mathcal{D}_{MG} = (N^t_{g,c} - \sum_{k\neq n_u}^{N_{g,n_u}} N^{r_k}_{g,c}) \times \min(M,\ T). \tag{27}$$

The minimum diversity order is achieved, when the total number of antenna arrays in the user group is equal to the corresponding total number of transmit antenna arrays, e.g. $N^t_{g,c} = \sum_{k=1}^{N_{g,n_u}} N^{r_k}_{g,c}$. The diversity order is then reduced to that of a single-user STSK system [9] associated with $(N^t_{g,c} - \tilde{\mathcal{R}}_{BD,n_u}) = M = N^{r_k}_{g,c}$, hence we have $\min(\mathcal{D}_{MG}) = N^{r_k}_{g,c} \times \min(M,\ T)$.

F. SYSTEM THROUGHPUT

The Cyclic Prefix (CP) reduces the throughput of the system [22], especially at mmWaves, where the CP is substantially higher compared to the systems operating in lower frequency bands. According to [27], each STSK codeword carries $\log_2(M_q M_c)$ bits and the achievable throughput per user is defined as

$$R_c = \frac{\log_2(M_q M_c)}{\left(1 + \frac{N_{cp}}{N_{sc}}\right)}\,(bit/symbol), \tag{28}$$

where a large value of N_{cp} drastically reduces the attainable throughput. However, due to the large bandwidth available at each of the mmWave frequency bands, the total bandwidth can be further divided into a large number of narrowband sub-channels. For example, assuming a 1 GHz bandwidth in the 28 GHz frequency band that can be divided into $N_{sc} = 4096$ or $N_{sc} = 8192$ sub-bands, which reduces the effect of a 100-symbol CP. Furthermore, at 60 GHz, the number of data-bearing sub-carriers may be an order of magnitude higher than the CP length, hence for $N_{sc} \gg N_{cp}$ (28) can be written as

$$[R_c]_{\frac{N_{cp}}{N_{sc}} \approx 0} \rightarrow \log_2(M_q M_c)\,(bit/symbol). \tag{29}$$

III. RESULTS

In this section the performance of the LMG-SSTSK system is evaluated using Monte Carlo simulations.

Consider a single-group based system supporting $K = 4$ users, where the transmitter constructs a single-layer in our LMG-SSTSK system. The BER performance of this system is shown in Figure 6,

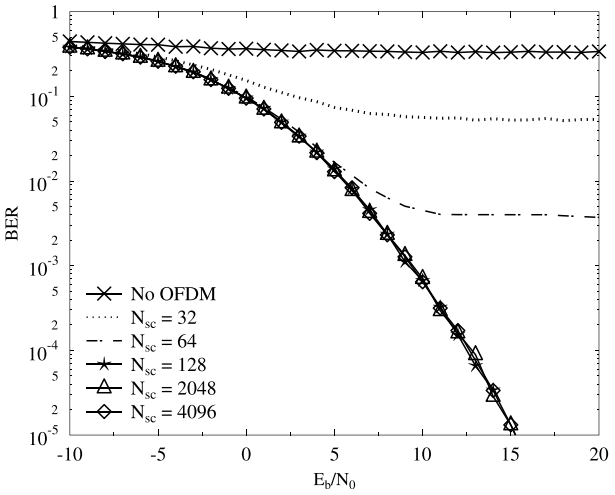

FIGURE 6. BER performance of uncoded LMG-SSTSK(8, 2, 2, 2, 4, 4) for $K = 4$ users and $N_{sc} = 32$, 64, 128, 2048 and 4096 sub-carriers for transmission over the mmWave channel. The performance of the basic single-carrier STSK(2,2,2,4,4) scheme operating without OFDM is shown in (×).

where the LMG-SSTSK(8, 2, 2, 2, 4, 4) arrangement relying on QPSK modulation and different number of sub-carriers, namely on $N_{sc} = 32, 64, 128, 2048$, and 4096 sub-carriers, is evaluated for transmission over the mmWave channel. Other system configurations, such as the distance, transmit power, directional antenna gains, receiver configurations and channel characteristics are shown in Table 1. The curve characterizing the performance of the basic STSK(2,2,2,4,4) single-carrier scheme is represented by the (×) marker.

TABLE 1. System Parameters for LMG-SSTSK.

Parameters	Values
Carrier Frequency	28 GHz
Bandwidth	500 MHz
P_t	30 dB
$N^t_{c,g}$	16
$N^{r_{n_u}}_{c,g}$	2
G_{Rx}	24 dBi
G_{Tx}	24 dBi
System	LMG-SSTSK
N_{sc}	2048
N_{cp}	100
Distance	78 m
N_{cl}	Poiss($\mu = 3.4$, $\sigma = 2.1$)
$N_p(n_c)$	Exp($\mu = 66.3$, $\sigma = 68.0$)
RMS DS	Exp($\mu = 13.4$, $\sigma = 11.5$)
AoA, AoD, AS	Exp($\mu = 34.6$, $\sigma = 27.8$)
$\bar{\varphi}^{Rx}$ and $\bar{\varphi}^{Tx}$	U(0, 360)

As shown in Figure 6, the performance of the system communicating over the mmWave channel is dependent on the number of sub-carriers used. For $N_{sc} = 32$ and 64 sub-carriers, we encountered an error floor similar to the

single-user OFDM-STSK system relying on a small number of sub-carriers in [27]. However, when dividing the bandwidth into a higher number of sub-channels, such as $N_{sc} \geq 128$, the system attains a BER of 10^{-5} at an E_b/N_0 of 16 dB. Since by dividing a huge BW, e.g. 500 MHz, into small number of sub-channels, each sub-channel would be wide enough to introduce ISI. Hence, the total system bandwidth should be divided into a large number of narrowband sub-channels in order to overcome the dispersive channel's ISI.

In the following, we scale-up the system to a multi-layered LMG-SSTSK system, where the key parameters summarizing the system characteristics used for the Monte Carlo simulation are listed in Table 1.

In our simulations, a base station equipped with 64 antenna arrays communicates with $K = 20$ users at 28 GHz carrier frequency, each provided with $N_{c,g}^{r_{nu}} = 2$ antenna arrays. The LMG-SSTSK system divides the total number of $K = 20$ users into 4 groups, where $N_{g,c}^{t} = 16$ antenna arrays per layer are dedicated to serve each user group. Sub-dividing the users into groups enables the system to communicate with all the $K = 20$ users in the group instead of only with the users of a single group at a time. The four groups $\{G_1, G_2, G_3, G_4\}$ have 2, 4, 6 and 8 users, and STSK(2,2,2,4,4) encoders are used to convey the information to all users.[9] *Based on Equation (28), the achievable throughput of the system over* $T = 2$ *time slots is equal to* $\frac{\log_2(16)}{\left(1+\frac{100}{2048}\right)} = 3.81$ *bits/symbol.*

Initially, the system is simulated under the assumption of having no ABF gain and no second stage BBP, where the BD is adopted for MU-TPC. Owing to the fact that the number of components of the g-th antenna array should be higher than or equal to the total number of receive antenna arrays in the g-th user group, and under the constraint of having $N_{c,g}^{r_{nu}} = M$, the simulated system can handle a maximum of 8 users per group. The BER performance of this LMG-SSTSK system is shown in Figure 7. Given that all antenna layers are of the same dimension, the BER performance is enhanced as the number of users decreases, i.e. $BER_{G_1} > BER_{G_2} > BER_{G_3} > BER_{G_4}$. The BER performance in G_1 is equivalent to that of the STSK(2,2,2,4,4) system [9], since this group is formed of 8 users, which is the maximum number of users per antenna layer. Furthermore, based on Equation (27), the diversity order achieved in G_1 is $\mathcal{D}_{MG} = (16 - 14) \times \min(2 \times 2) = 4$, which is equal to the diversity order of the STSK(2,2,2,4,4) system in Figure 7. Given the identical antenna layer dimensions, a higher diversity order can be achieved in the specific user groups accommodating a smaller number of users. Observe from Equation (27) that the diversity orders of groups G_2, G_3 and G_4 are 12, 20 and 28, which are equal to the diversity orders of STSK(2,6,2,4,4), STSK(2,10,2,4,4) and STSK(2,14,2,4,4), respectively, as seen in Figure 7.

In Figure 8, the BER performance of a single user in G_3 is shown compared to the performance recorded after employing second-stage BBP-MMSE precoding and ABF using different antenna array sizes at the transmitter and receiver; e.g. $N_{AA}^{t} = 2$ and 4 and $N_{AA}^{r_{nu}} = 2$. The system shows that applying a second stage BBP does not enhance the attainable BER performance of the system, but it reduces the computational cost of the ML detector and reduces the receiver's design complexity. The BER achievable performance may be further enhanced with the aid of ABF by employing multiple AEs at each of the antenna arrays at both the transmitter and receivers.

[9]Note that the poposed system can work with any number of users and any number of antennas while using any STSK configuration.

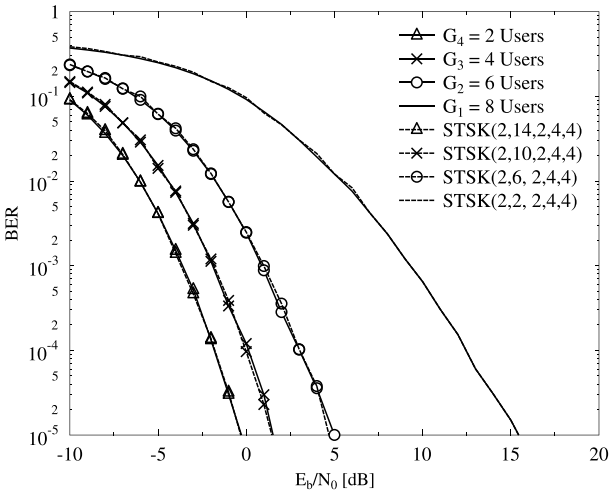

FIGURE 7. The BER performance of LMG-SSTSK(64, 2, 2, 2, 4, 4) in conjunction with 64 single-element antenna arrays, sub-divided into four groups each with 16 single-antenna arrays for transmission over the 28 GHz channel, adopted to serve four groups each with 8,6,4,and 2 users.

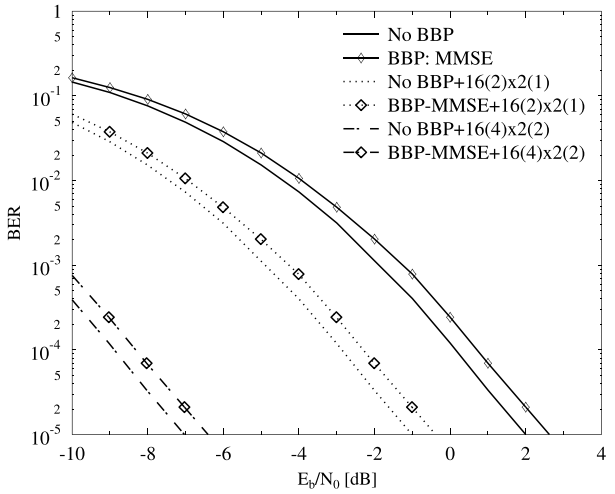

FIGURE 8. The BER performance of LMG-SSTSK(64, 2, 2, 2, 4, 4) system within a single group with $N_{g,u} = 4$ users compared to its performance enhanced by second-stage MMSE precoding and different antenna array sizes at the transmitter and receiver; e.g. $N_{AA}^{t} = 2$, *and* 4 and $N_{AA}^{r_{nu}} = 2$.

IV. CONCLUSIONS

The OFDM-aided MG-MIMO concept was proposed for mmWaves systems. This system is capable of enhancing the MU-MIMO efficiency in terms of the number of

simultaneously served users when operating at mmWaves. Owing to their high attenuation, mmWave signals cannot reach distant users at the same time with the same transmit beam. Hence, as a solution, all users are divided into groups and the transmit antenna arrays are divided into array layers for supporting the user groups. Furthermore, when the number of users detected in a group is lower than the maximum number of users, a higer diversity order is achieved with the aid of the additional antenna arrays.

The proposed system may be used as the basis of multi-group system, where multiple MIMO techniques may be combined into layers in order to form the LMG scheme.

REFERENCES

[1] L. Hanzo, H. Haas, S. Imre, D. O'Brien, M. Rupp, and L. Gyongyosi, "Wireless myths, realities, and futures: From 3G/4G to optical and quantum wireless," *Proc. IEEE*, vol. 100, no. Special Centennial Issue, pp. 1853–1888, May 2012.

[2] T. S. Rappaport *et al.*, "Millimeter wave mobile communications for 5G cellular: It will work!" *IEEE Access*, vol. 1, pp. 335–349, May 2013.

[3] P. A. Tenerelli and C. W. Bostian, "Measurements of 28 GHz diffraction loss by building corners," in *Proc. 9th IEEE Int. Symp. Pers., Indoor Mobile Radio Commun.*, vol. 3. Sep. 1998, pp. 1166–1169.

[4] S. Alamouti, "A simple transmit diversity technique for wireless communications," *IEEE J. Sel. Areas Commun.*, vol. 16, no. 8, pp. 1451–1458, Oct. 1998.

[5] P. W. Wolniansky, G. J. Foschini, G. D. Golden, and R. A. Valenzuela, "V-BLAST: An architecture for realizing very high data rates over the rich-scattering wireless channel," in *Proc. Int. Symp. Signals, Syst., Electron. (ISSSE)*, Sep./Oct. 1998, pp. 295–300.

[6] L. Hanzo, M. El-Hajjar, and O. Alamri, "Near-capacity wireless transceivers and cooperative communications in the MIMO era: Evolution of standards, waveform design, and future perspectives," *Proc. IEEE*, vol. 99, no. 8, pp. 1343–1385, Aug. 2011.

[7] L. L. Hanzo, O. Alamri, M. El-Hajjar, and N. Wu, *Near-Capacity Multi-Functional MIMO Systems: Sphere-Packing, Iterative Detection and Cooperation*. New York, NY, USA: Wiley, 2009. [Online]. Available: http://books.google.co.uk/books?id=590-JItOJREC

[8] M. El-Hajjar, O. Alamri, J. Wang, S. Zummo, and L. Hanzo, "Layered steered space-time codes using multi-dimensional sphere packing modulation," *IEEE Trans. Wireless Commun.*, vol. 8, no. 7, pp. 3335–3340, Jul. 2009.

[9] S. Sugiura, S. Chen, and L. Hanzo, "Space-time shift keying: A unified MIMO architecture," in *Proc. IEEE Global Telecommun. Conf.*, Dec. 2010, pp. 1–5.

[10] O. El Ayach, S. Rajagopal, S. Abu-Surra, Z. Pi, and R. W. Heath, Jr., "Spatially sparse precoding in millimeter wave MIMO systems," *IEEE Trans. Wireless Commun.*, vol. 13, no. 3, pp. 1499–1513, Mar. 2014.

[11] J. Brady, N. Behdad, and A. M. Sayeed, "Beamspace MIMO for millimeter-wave communications: System architecture, modeling, analysis, and measurements," *IEEE Trans. Antennas Propag.*, vol. 61, no. 7, pp. 3814–3827, Jul. 2013.

[12] J. Nam, J. Y. Ahn, A. Adhikary, and G. Caire, "Joint spatial division and multiplexing: Realizing massive MIMO gains with limited channel state information," in *Proc. 46th Annu. Conf. Inf. Sci. Syst.*, Mar. 2012, pp. 1–6.

[13] A. Adhikary, J. Nam, J. Y. Ahn, and G. Caire, "Joint spatial division and multiplexing—The large-scale array regime," *IEEE Trans. Inf. Theory*, vol. 59, no. 10, pp. 6441–6463, Oct. 2013.

[14] S. Sun, T. S. Rappaport, R. W. Heath, Jr., A. Nix, and S. Rangan, "MIMO for millimeter-wave wireless communications: Beamforming, spatial multiplexing, or both?" *IEEE Commun. Mag.*, vol. 52, no. 12, pp. 110–121, Dec. 2014.

[15] S. Sun, G. R. MacCartney, Jr., M. K. Samimi, S. Nie, and T. S. Rappaport, "Millimeter wave multi-beam antenna combining for 5G cellular link improvement in New York City," in *Proc. IEEE Int. Conf. Commun. (ICC)*, Jun. 2014, pp. 5468–5473.

[16] Z. Pi and F. Khan, "An introduction to millimeter-wave mobile broadband systems," *IEEE Commun. Mag.*, vol. 49, no. 6, pp. 101–107, Jun. 2011.

[17] W. Roh *et al.*, "Millimeter-wave beamforming as an enabling technology for 5G cellular communications: Theoretical feasibility and prototype results," *IEEE Commun. Mag.*, vol. 52, no. 2, pp. 106–113, Feb. 2014.

[18] S. Rangan, T. S. Rappaport, and E. Erkip, "Millimeter-wave cellular wireless networks: Potentials and challenges," *Proc. IEEE*, vol. 102, no. 3, pp. 366–385, Mar. 2014.

[19] Q. H. Spencer, A. L. Swindlehurst, and M. Haardt, "Zero-forcing methods for downlink spatial multiplexing in multiuser MIMO channels," *IEEE Trans. Signal Process.*, vol. 52, no. 2, pp. 461–471, Feb. 2004.

[20] Y. Xu, G. Yue, N. Prasad, S. Rangarajan, and S. Mao, "User grouping and scheduling for large scale MIMO systems with two-stage precoding," in *Proc. IEEE Int. Conf. Commun. (ICC)*, Jun. 2014, pp. 5197–5202.

[21] M. K. Samimi and T. S. Rappaport, "Ultra-wideband statistical channel model for non line of sight millimeter-wave urban channels," in *Proc. IEEE Global Commun. Conf. (GLOBECOM)*, Dec. 2014, pp. 3483–3489.

[22] M. I. Kadir, S. Sugiura, J. Zhang, S. Chen, and L. Hanzo, "OFDMA/SC-FDMA aided space–time shift keying for dispersive multiuser scenarios," *IEEE Trans. Veh. Technol.*, vol. 62, no. 1, pp. 408–414, Jan. 2013.

[23] A. Ghosh, R. Ratasuk, B. Mondal, N. Mangalvedhe, and T. Thomas, "LTE-advanced: Next-generation wireless broadband technology [Invited Paper]," *IEEE Wireless Commun.*, vol. 17, no. 3, pp. 10–22, Jun. 2010.

[24] Q. H. Spencer, C. B. Peel, A. L. Swindlehurst, and M. Haardt, "An introduction to the multi-user MIMO downlink," *IEEE Commun. Mag.*, vol. 42, no. 10, pp. 60–67, Oct. 2004.

[25] M. R. Akdeniz *et al.*, "Millimeter wave channel modeling and cellular capacity evaluation," *IEEE J. Sel. Areas Commun.*, vol. 32, no. 6, pp. 1164–1179, Jun. 2014.

[26] M. K. Samimi and T. S. Rappaport, "3-D statistical channel model for millimeter-wave outdoor mobile broadband communications," in *Proc. IEEE Int. Conf. Commun. (ICC)*, Jun. 2015, pp. 2430–2436. [Online]. Available: http://arxiv.org/abs/1503.05619

[27] M. I. Kadir, S. Sugiura, S. Chen, and L. Hanzo, "Unified MIMO-multicarrier designs: A space–time shift keying approach," *IEEE Commun. Surveys Tuts.*, vol. 17, no. 2, pp. 550–579, Nov. 2015.

IBRAHIM A. HEMADEH received the B.Eng. (Hons.) degree in computer and communications engineering from the Islamic University of Lebanon, in 2010, and the M.Sc. (Hons.) degree in wireless communications from the University of Southampton, U.K., in 2012, where he is currently pursuing the Ph.D. degree in wireless communications under the supervision of Prof. L. Hanzo and Dr. M. El-Hajjar. His research interests mainly include millimeter wave communications, multi-functional MIMO, and multiuser MIMO.

MOHAMMED EL-HAJJAR received the B.Eng. degree in electrical engineering from the American University of Beirut, Lebanon, in 2004, and the M.Sc. degree in radio frequency communication systems and the Ph.D. degree in wireless communications from the University of Southampton, U.K., in 2005 and 2008, respectively. He joined Imagination Technologies as a Design Engineer, where he worked on designing and developing imagination's multistandard communications platform, which resulted in three patents. In 2012, he joined the Electronics and Computer Science Department, University of Southampton, as a Lecturer with the Southampton Wireless Research Group. He is a Lecturer with the Electronics and Computer Science Department, University of Southampton. He has published a Wiley-IEEE book and in excess of 60 journal and international conference papers. His research interests are mainly in the development of intelligent communications systems, including energy-efficient transceiver design, MIMO, millimeter wave communications, and radio over fiber systems. He is a recipient of several academic awards, including the Dean's Award for creative achievement, the Dorothy Hodgkin Postgraduate Award, and the IEEE ICC 2010 Best Paper Award.

SEUNGHWAN WON (M'04) received the B.S. and M.S. degrees in radio science and engineering from Korea University, Seoul, South Korea, in 1999 and 2001, respectively. He is currently pursuing the Ph.D. degree with the Communications Research Group, School of Electronics and Computer Science, University of Southampton, U.K. He was a Research Engineer with the Mobile Communication Technology Research Laboratory, LG Electronics R&D, from 2001 to 2004. He was a recipient of the 2004 state scholarship of the Information and Telecommunication National Scholarship Program, Ministry of Information and Communication (MIC), South Korea. His major research interests included initial synchronization in noncoherent MIMO aided single- and multi-carrier CDMA, IDMA, and OFDMA as well as in iterative synchronization schemes designed for MIMO aided single- and multi-carrier transmission systems. He published a host of papers in these research fields. Upon completing his Ph.D., he returned to his native Korea and joined Samsung. In 2013, he was appointed as an Associate Professor with the University of Southampton and currently he is teaching and conducting research with the University of Southampton in Johor, Malaysia.

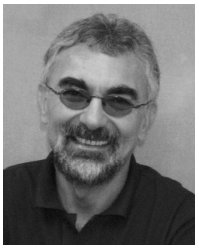

LAJOS HANZO received the degree in electronics in 1976, the doctorate degree in 1983, and the Doctor Honoris Causa degree from the Technical University of Budapest, in 2009. During his 38-year career in telecommunications, he has held various research and academic posts in Hungary, Germany, and the U.K. Since 1986, he has been with the School of Electronics and Computer Science, University of Southampton, U.K., where he holds the Chair in Telecommunications. He has successfully supervised about 100 Ph.D. students, co-authored 20 John Wiley/IEEE Press books on mobile radio communications totaling in excess of 10 000 pages, published 1500+ research entries at the IEEE Xplore, acted both as the TPC and General Chair of the IEEE conferences, presented keynote lectures, and has been awarded a number of distinctions. He is currently directing a 100-strong academic research team, working on a range of research projects in the field of wireless multimedia communications sponsored by the industry, the Engineering and Physical Sciences Research Council, U.K., the European Research Council's Advanced Fellow Grant, and the Royal Society's Wolfson Research Merit Award. He is an Enthusiastic Supporter of industrial and academic liaison and he offers a range of industrial courses.